Desalination and Water Treatment
www.deswater.com
doi: 10.5004/dwt.2021.27569

241 (2021) 269–275
November

The impact of industrial pollution on urban groundwater resources

Dongling Cheng

College of Water Resources and Architectural Engineering, Northwest A&F University, Yangling 712100, China, email: dolingcheng11@163.com

Received 25 June 2021; Accepted 23 September 2021

ABSTRACT

To promote the sustainable development of groundwater resources in China and form an environment where industry and resources coexist harmoniously, industrial pollution causes large emissions, wide pollution ranges, and difficult treatment of groundwater resources to be further alleviated. The water resources research digital model and the MODFLOW model are selected to carry out the research on the current situation of groundwater resources pollution, and the water pollution situation of Plant A is selected as a research example. Firstly, through the collection and analysis of a large number of samples, the characteristics of groundwater pollution in Plant A are revealed. Secondly, combined with field geological surveys and hydrogeological tests, the hydrogeological conditions of the study area and the nitrogen fertilizer plant are ascertained. Finally, according to the verified solute transport model analysis, the pollution law of the characteristic pollutant (ammonia nitrogen) in the loose groundwater of the contaminated site of the nitrogen fertilizer plant is studied. The results of the study show that pollutants migrate slowly in the impermeable layer of surface silty clay, and the diffusion of pollutants is mainly vertical. The concentration of pollutants has a significant effect on the diffusion rate. The higher the concentration of pollutants is, the faster the diffusion rate is. In the vertical direction, the pollutant diffusion rate is also related to the pollutant carrier. The continuous leakage of wastewater is faster than the rainfall infiltration method. After the pollutants enter the deep silty sand confined aquifer, the pollutants accelerate to the direction of lower hydraulic gradient, and the migration speed shows a trend of uniform diffusion. Therefore, the groundwater pollution research is provided with new reference and reference materials, and the pollution problem of groundwater resources in China can be further alleviated.

Keywords: Industrial pollution; Groundwater; Simulation experiments; MODFLOW

1. Introduction

Water is the source of the growth of all things and the basic guarantee for the survival and development of human society. As an important part of water resources, groundwater resources have the characteristics of good water quality, abundant reserves, and convenient exploitation. Groundwater resources are the main source of water needed for the development of modern industry. Especially in recent years, with the rapid development of social science and technology, the process of industrialization has been accelerating. The quality of groundwater is continuously affected by various human and natural factors, which has caused groundwater resources to face an increasingly serious environmental crisis. Especially the "three wastes" discharged from industrial production and the wastewater produced in people's daily life have a relatively large impact on the quality of groundwater. Meanwhile, the excessive use of chemical fertilizers and pesticides in the agricultural production process, unreasonable mining and other human factors have a particularly prominent impact on the quality of groundwater. A lot of pollutants produced

by the above process enter the groundwater system, which causes the pollution of groundwater resources to exceed its own ability to regulate and restore. Then, groundwater quality deteriorated sharply and reserves continued to decrease, and eventually the natural balance of groundwater resources is broken [1,2].

Judging from the current development situation, if certain protection measures are not taken for groundwater resources, various human and natural factors will have an increasingly serious impact on groundwater resources. Meanwhile, groundwater resources have particularities, such as the hidden complexity of burial, slow self-flow rate and weak self-purification ability. Therefore, once groundwater resources are polluted, the difficulty of governance will be far more difficult than that of surface water, the governance cost will also very high, and the governance effect will take a long time to achieve [3,4].

The digital model of water resources research and the MODFLOW model are selected to carry out research on the current status of groundwater resources pollution. Water pollution situation of Plant A is selected as a research example, and the impact of industrial pollution on groundwater resources is shown in detail. The research has made innovations in the following aspects: (1) A comprehensive and systematic simulation study of the groundwater flow field in Plant A has been carried out. The MODFLOW model and digital processing methods are used to carry out detailed analysis of the groundwater resources pollution in Plant A, which lays the foundation for the research on the impact of industrial pollution on groundwater resources. (2) Combined with related simulation experiments, the pollution of groundwater caused by ammonia nitrogen is refined, which makes the research content more subdivided.

2. Methods

2.1. MODFLOW Model

Canadian Hydrogeology Company developed a software called Visual MODFLOW. This software builds a systematic Windows menu interface based on various software such as MODFLOW, RT3D, WINPEST, MT3D99, and MODPATH, and has a visualization function [5]. The biggest advantage of this software is its simplicity, powerful functions, reasonable and scientific menu structure, convenient and practical visual interactive interface, which can well support the input and output of the model. Therefore, this software is used by many groundwater simulation workers as the first choice for simulating groundwater environment [6,7].

To study the groundwater flow field and the movement law of pollutants, the three-dimensional visual groundwater flow model established by Visual MODFLOW is used to study the selected area.

2.1.1. Groundwater Flow Model

According to the analysis and investigation of the study area, the area is a relatively independent groundwater system. In this simulation, field investigations and evaluations are carried out, and then the groundwater flow system is initially recognized and analyzed. The groundwater discharged from Plant A industrial production flows into the regional reservoir. The groundwater in the solid waste area, hazardous material storage area, recycled metal dismantling area, and anode copper refining area flow into the Luo River, so the two belong to different hydrogeological units. Therefore, this simulation is divided into simulated Area A and simulated Area B. Fig. 1 shows the range of the simulated Area A, which has an area of 3.41 km^2. Fig. 2 shows the range of the simulated Area B, which has an area of 2.5 km^2.

The aquifers in the simulation area are mainly Quaternary loose pore water and bedrock fissure water. The entire simulation area is generalized as a single-layer diving. Quaternary loose pore phreatic water and bedrock fissure water are generalized into two different types of single-layer phreatic water. Therefore, in this evaluation, Quaternary phreatic aquifers and bedrock fissure water aquifers are designated as the target aquifers for simulation and prediction, and generalized into heterogeneous and continuous aquifers. Quaternary phreatic aquifers and bedrock fissure water aquifers are mainly recharged by natural precipitation and lateral recharge from the piedmont [8–10]. Based on the field survey and indoor analysis of hydrogeology, the simulated Area A and B are in two different hydrogeological units. From the watershed to the front of the mountain, there are neither towns, villages, nor large water intake projects. The lateral recharge is only the natural precipitation that penetrates vertically into the fissures of the bedrock and meanwhile discharges to the groundwater area [11]. The equation is as follows.

$$D = 0.1 \times S \times R \times p \tag{1}$$

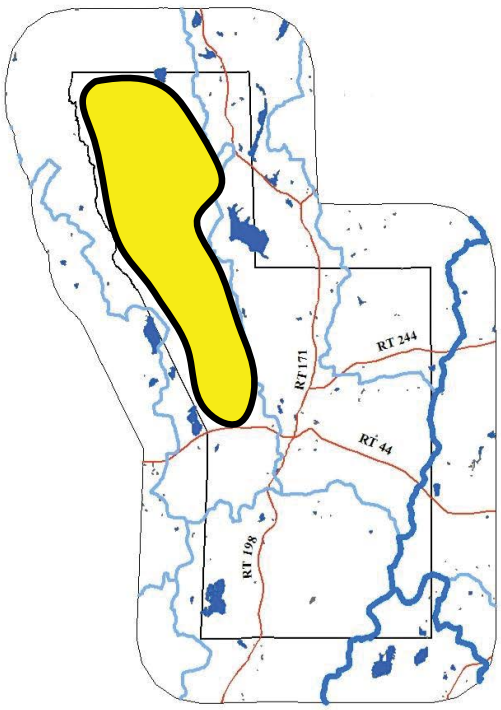

Fig. 1. The range of the simulated area A.

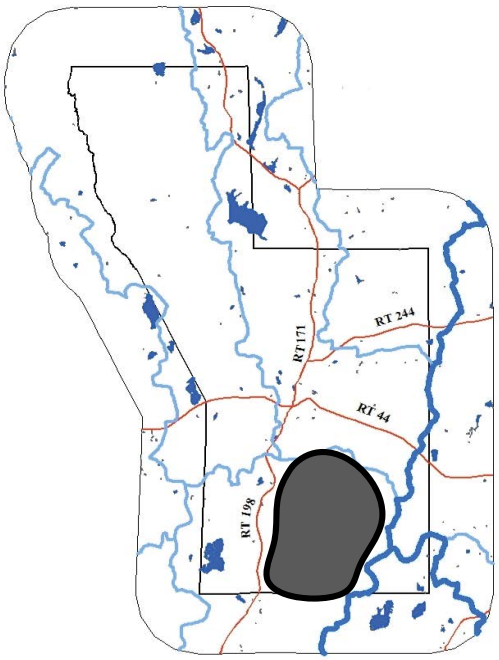

Fig. 2. The range of the simulated area B.

where D is the volume of atmospheric precipitation infiltrated and recharged (ten thousand square meters per year), and S is the calculated area (square kilometres). R is the annual average rainfall (mm), and p is the rainfall infiltration coefficient.

Fig. 3 shows the lateral recharge of the simulated Area A and B after calculation.

In the above data, the simulated Area A adopts a calculation area of 2.11 km^2, and its lateral recharge volume is 32,100 m^3/y. The simulated Area B has a calculated area of 2.85 km^2, and the lateral recharge volume is 43,300 m^3/y. The positive correlation between the area and the lateral recharge volume can be initially confirmed. That is, the larger the area, the greater the recharge volume.

2.1.2. Model of solute transport

According to the groundwater flow field of the phreatic aquifer and the movement of pollutants, the adsorption, exchange, biological reaction, and chemical reaction of pollutants in the aquifer are not considered. The mathematical model of solute transport in groundwater can be expressed as follows.

$$m_e = \frac{\alpha D}{\alpha u} = \frac{\alpha}{\alpha x_j}\left(m_e E_{jk}\frac{\alpha D}{\alpha x_k}\right) - \frac{\alpha}{\alpha x_j}\left(m_e D W_j\right) \pm DY \tag{2}$$

$$E_{jk} = \beta_{ijmn}\frac{W_m W_n}{|W|} \tag{3}$$

where β_{ijmn} is the dispersion of the aquifer, and W_m and W_n are the velocity components in the direction respectively. $|W|$ is the velocity modulus, and D is the concentration of

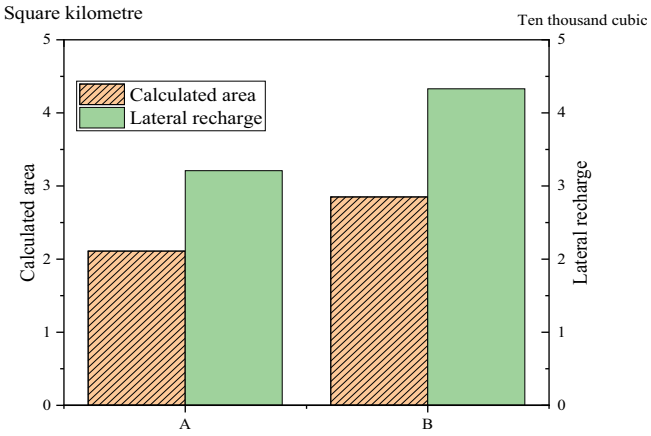

Fig. 3. Lateral recharge.

the simulated pollutant (mg/L). m_e is the effective porosity, u is the time, and D' is the source and sink concentration of the simulated pollutant (mg/L). Y is the flux per unit area of the source and sink, and W_j is the seepage velocity (m/d).

2.2. Digital model

Through analysis, the regional hydrogeological conditions of Plant A and the entire basin is studied. The groundwater flow in Plant A is generalized into a stable, homogeneous and anisotropic groundwater flow system, and generalized analysis is carried out through the following mathematical model.

Eq. (4) shows that the groundwater type of Plant A is mainly pore confined aquifers, and the equation of the steady flow of groundwater in the three-dimensional confined water aquifer is generalized and analyzed.

$$\frac{\partial}{\partial x}\left(S_{\text{mm}}\frac{\partial h}{\partial x}\right) + \frac{\partial}{\partial y}\left(S_{\text{nn}}\frac{\partial h}{\partial y}\right) + \frac{\partial}{\partial z}\left(S_{\text{oo}}\frac{\partial h}{\partial z}\right) + P = W_K\frac{\partial h}{\partial t} \tag{4}$$

where S_{mm} is the main value of the permeability coefficient in the m direction, and m/d and S_{nn} are the main values of the permeability coefficient in the n direction. m/d and S_{oo} are the main values of the permeability coefficient in the o direction, m/d and W_K are the elastic water release coefficients, and P is the recharge intensity in the vertical direction [12,13].

2.2.1. Meshing

The entire area of Plant A is regarded as the main research object. In the vertical direction, the Quaternary strata are generalized into three layers: silty clay layer, sand gravel layer and clay layer. The sand-gravel aquifer is the main research object of this simulation. Fig. 4 shows a schematic diagram of the network dissection of the hydrogeological unit model.

The Quaternary system of the entire basin is generalized into a simulation area of 18,177 × 17,851 m. Firstly, the simulation area is divided into 100 × 100 × 3 cells for simulation research. Secondly, the model boundary conditions,

source and sink terms, permeability coefficients, water supply and other hydrogeological parameters are imported into the three-dimensional finite-difference grid model. Finally, the mathematical model of the groundwater three-dimensional steady flow field in the study area is established.

2.2.2. Source and sink items

The recharge source of groundwater in Plant A mainly receives recharge from atmospheric rainfall. The carbonate rock fractured karst water in the surrounding mountainous area will be fed to the aquifer in the basin through the fractured karst channel along the hydraulic gradient. According to the multi-year rainfall data provided by the weather station, the annual average rainfall of the local rainy season is 815.8 mm. According to 200,000 hydrogeological survey reports and statistical data, the rainfall infiltration coefficient in this area is 0.03~0.25. Combined with the regional average rainfall and rainfall infiltration coefficient, the rainfall infiltration recharge in the region ranges from 0.000071 to 0.00588 m/d.

Based on the different rainfall in different periods, the groundwater level also varies in different seasons. The actual observation level of regional groundwater is an important basis for verifying the accuracy of the model. The field work period is in April, and the water level is from the dry season to the normal season. Therefore, the selected rainfall infiltration recharge is slightly smaller and adjusted to 0.0026 m/d.

In addition to atmospheric rainfall, the source of the Quaternary pore water recharge in the basin also receives lateral runoff recharge from the karst water in the carbonate fractures in the mountainous areas surrounding the basin. Darcy's Eq. (5) shows the calculation of lateral runoff recharge [14].

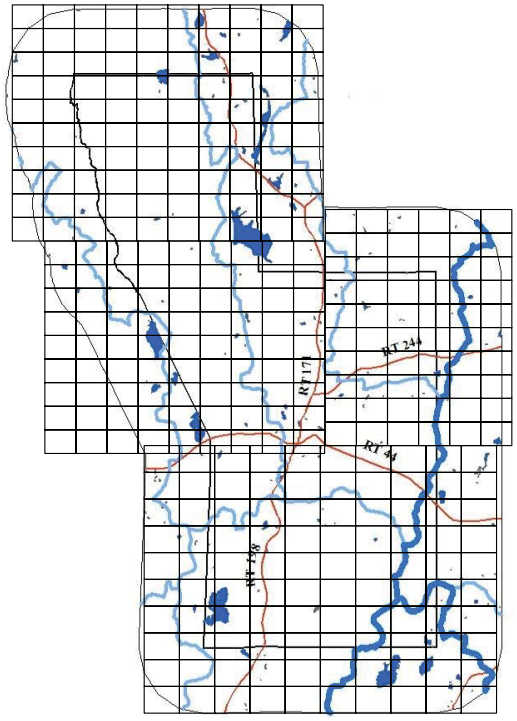

Fig. 4. Network dissection of the hydrogeological unit model of plant A.

$$C = PDHZ \tag{5}$$

In the formula, C is the lateral runoff recharge, and m^3 and P are the average permeability coefficients of the profile aquifer. m/d and D are the average hydraulic gradient of groundwater, dimensionless. H is the thickness of the aquifer, m and Z are the length of the section perpendicular to the direction of groundwater flow. Table 1 shows that according to the calculation, the calculation results of the inner recharge volume in the Area A and B are obtained.

From the above data, the groundwater in the region mainly receives lateral recharge from the karst water in the carbonate fractures in the west, south, east and northeast. The permeability coefficient, hydraulic slope, and cross-sectional length of Area A are smaller than those of Area B, but the thickness of the aquifer is higher than that of Area B. The final actual comprehensive water recharge volume is 320.7864 in Area A, 876.0276 in Area B, and the total recharge volume in all areas is 1196.814.

2.2.3. Hydrogeological parameters

Due to differences in regional functions and pollution conditions, infiltration conditions are also different. Fig. 5 shows the sediment types and thickness of the specific infiltration in the study area.

Based on the data in Fig. 5, combined with the specific regional geology, it can be analyzed that the surrounding areas are mainly sand and gravel. The central particles gradually become smaller and become excessively fine sand and silt sand. Therefore, the permeability coefficients of various internal blocks also show certain differences. In the process of groundwater numerical simulation, each block needs to be assigned a permeability coefficient that can reflect the different permeability of each block.

2.3. Analysis of industrial pollution sources

After consulting relevant information, the nitrogen fertilizer plant mainly uses coal as a raw material to produce nitrogen fertilizer and synthetic ammonia. Sulfuric acid and manganese ore are used as raw materials to produce manganese sulfate. Its production sewage, production waste residues and product leakage are all important sources of

Table 1
Calculation table of lateral recharge

Range	A	B
Average permeability coefficient (m/d)	2.2	2.4
Mean hydraulic gradient	0.0029	0.0053
Thickness of aquifer (m)	5	3.9
Length of section (m)	10,056	17,659
Recharge volume (m^3)	320.7864	876.0276

groundwater pollution in the plant. Fig. 6 shows the specific production process.

Fig. 6 shows that the synthetic ammonia production process is more complicated. It mainly includes three parts: gas generation stage, purification stage and synthesis stage. Each stage corresponds to a different production process, and the pollution sources and pollutants produced are also different. The process flow mainly uses coal as raw material to make coal water slurry. The crude water gas needed to synthesize ammonia under high temperature conditions is refined gas through a series of decarburization, desulfurization and copper washing treatments. Finally, the refined gas is compressed and reacted to form synthetic ammonia in the synthesis workshop [15]. The plant mainly uses coal as a raw material to produce synthetic ammonia and nitrogen fertilizer. Table 2 shows in detail the possible pollution links in different processes.

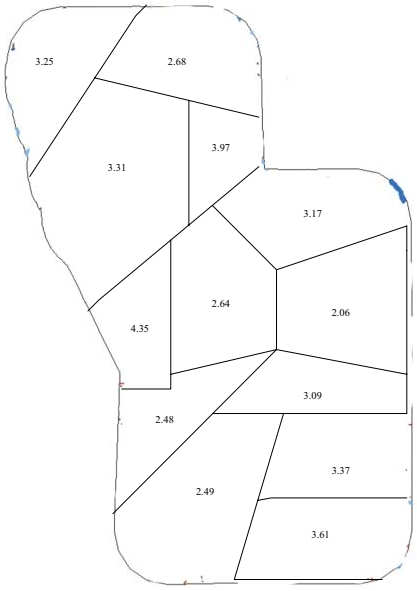

Fig. 5. Permeability coefficient in different areas.

Table 2 shows that the main pollutants in the groundwater are volatile phenol, ammonia nitrogen, sulfate and manganese. These four pollutants have been polluted to varying degrees in shallow and deep groundwater. Excessive ammonia nitrogen is more serious. During the synthesis of ammonia, different production processes correspond to different raw materials and products, and pollution sources and pollutants produced are also different [16–19].

3. Results and discussion

3.1. Simulation verification of ammonia nitrogen pollution source

In this simulation, a certain concentration of pollutant injection wells is set up in the form of point sources, which is equivalent to wastewater leakage. The continuous injection time of pollutants in this simulation is from the beginning of plant construction to the end of production shutdown, and from production shutdown to monitoring period through natural transport.

The amount of sewage leakage is set to 1 m^2/d, the ammonia nitrogen concentration of sewage in the synthesis workshop is set to 200 mg/L, and the ammonia nitrogen concentration of sewage in the gas plant is set to 150 mg/L. Figs. 7 and 8 show the comparison of the fitting situation.

The simulation results are compared with the actual monitoring results. In the first aquifer, the simulated concentrations of No. 1 and No. 2 boreholes are basically consistent with the monitoring results. In the second aquifer,

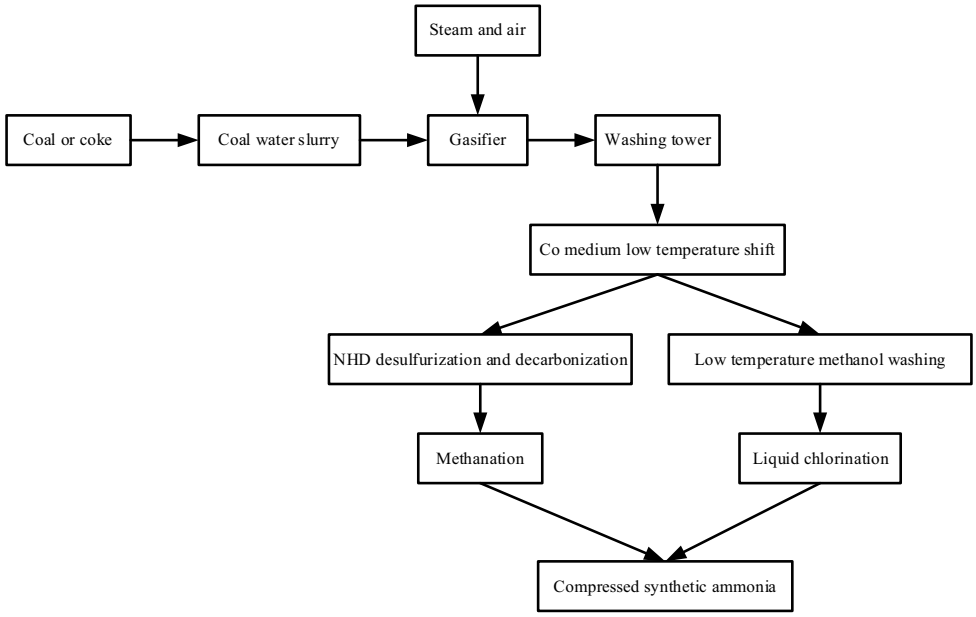

Fig. 6. Synthetic ammonia process.

Table 2
List of pollution production links

Process names	Production gas	Purge gas	CO conversion	Compression synthesis
Liquid pollution source	Gasification wastewater, also known as gray water (recycles, needs to be discharged intermittently to ensure water quality)	Process condensate (sent to sewage plant after stripping, or used in gas production process)	Conversion process condensate (strip to the sewage plant)	
Solid pollution source	Gasification ash	Waste catalyst	Waste catalyst in conversion section	Waste catalyst for ammonia synthesis

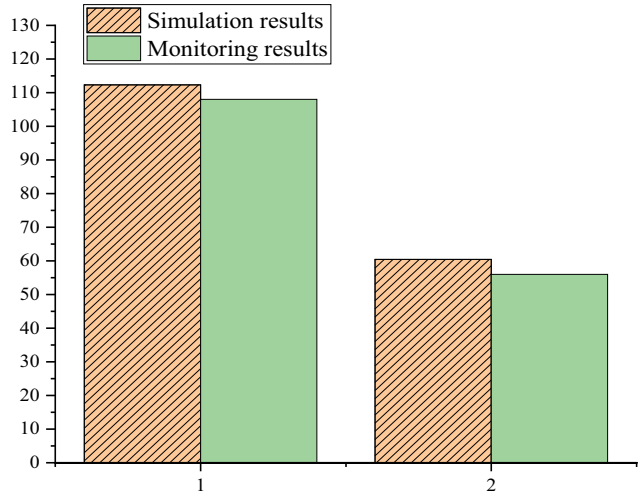

Fig. 7. Ammonia chloride pollution in the first aquifer wastewater leakage conditions.

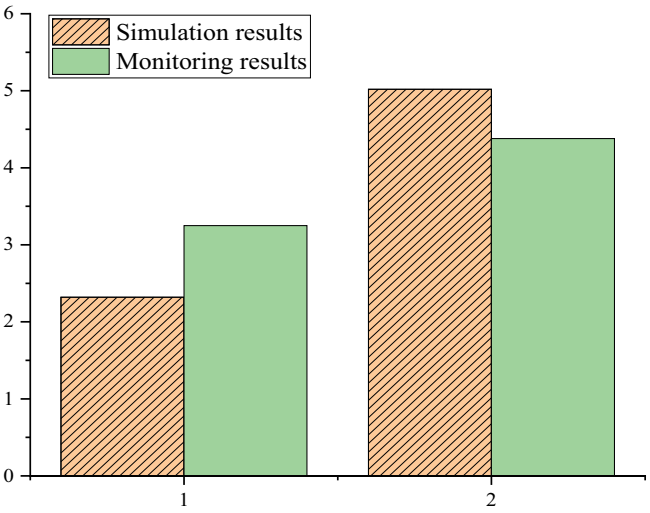

Fig. 8. Ammonia chloride pollution in the second aquifer wastewater leakage conditions.

the simulated concentrations of No. 1 and No. 2 are lower than the monitoring results, which are basically consistent with each other on the whole. Therefore, the set simulation conditions can represent the pollution status of the plant [20–22].

3.2. Migration law of pollutants in the continuous leakage of sewage

The ammonia nitrogen pollution condition of wastewater discharge at No. 1 and No. 2 in the original gas production workshop and synthesis workshop in the plant is compared and studied. The fitting concentration of ammonia nitrogen pollution is 150~200 mg/L. Through simulation analysis, the migration law of ammonia chloride pollutants in the silty clay aquifer is studied. Under the condition of continuous leakage of sewage, the migration speed of pollutants on the horizontal surface is relatively slow. From the fitted ammonia nitrogen pollutant solute transport model, different time periods from 800 to 8,000 d have diffused different distances. Fig. 9 shows the specific statistical results.

The diffusion statistics chart shows that in the silty clay medium, on the horizontal surface, as the diffusion range expands, the diffusion rate of pollutants becomes slower and slower. In 4,000 d, the ammonia nitrogen pollutants diffuse 60.08 m on the horizontal surface with an average diffusion rate of 0.015 m/d. Compared with the average vertical migration rate of 0.27 m/d, the pollutants mainly diffuse vertically.

4. Conclusion

The law of groundwater pollution in the contaminated site of the plant a is taken as the research target. Firstly, many samples are collected and analyzed, the characteristics of groundwater pollution in the plant are ascertained, and the source of pollution in the plant is analyzed. Secondly, combined with field geological surveys and hydrogeological tests, and simulation using GMS software, the pollution sources in the plant are verified. Finally, based on the verified solute transport model, the pollution law of groundwater in the contaminated site is analyzed and studied. The following conclusions are mainly obtained. The analysis results of the plant water samples show that in the shallow groundwater, ammonia nitrogen significantly exceeds the standard at No. 1 and No. 2, and ammonia nitrogen exceeds the standard at No. 1 abnormally. According to the distribution map of the production process of the plant, the southern part of the plant is the original plant waste slag dump. No. 1 and No. 2 are near the gas workshop, synthesis workshop, and manganese sulfate production plant. No. 2 is the warehouse for synthetic ammonia products in the plant. The groundwater pollution source of the site is mainly composed of three parts: product leakage, waste water discharge and waste residue. After the pollutants

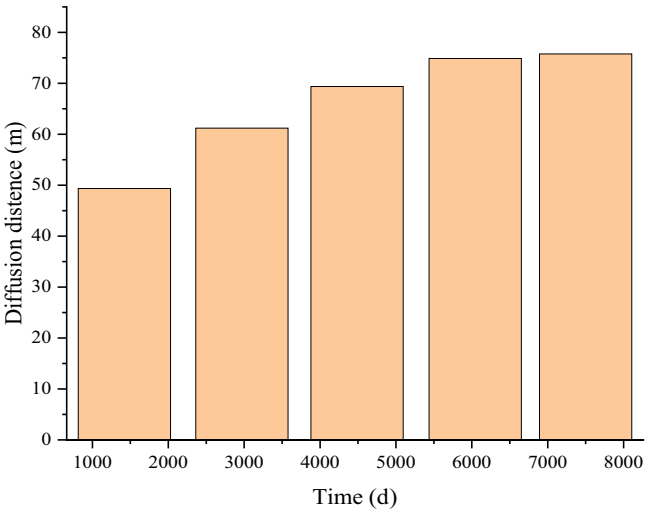

Fig. 9. Statistics of level diffusion of high-concentration ammonia nitrogen pollutants in silty clay layer.

enter the silty clay aquifer, the pollutants will accelerate migration in the direction of lower hydraulic gradient. The moving speed of s presents a uniform trend and has little relationship with the concentration of pollutants. The pollutants are mainly mechanically dispersed.

Subsequent research can be carried out around the following two points. (1) After the pollutants enter the silt aquifer, the main downstream direction is mechanical dispersion, so a lot of researches in pollution monitoring are needed. (2) Under high-concentration pollution conditions such as product leakage, the pollutant migration rate is faster, and the impact on groundwater is more obvious. Such production accidents should be avoided, and seepage prevention and emergency treatment should be done. The contaminated surface soil should be treated in time to avoid the continuous transfer of pollution.

References

[1] Z. Qu, Study on the characteristics of urban groundwater pollution and its control strategy, Energy Conserv., 39 (2020) 139–141.
[2] A.B. Mirajkar, P.L. Patel, Multiobjective two-phase fuzzy optimization approaches in management of water resources, J. Water Resour. Plann. Manage., 142 (2016) 166–167.
[3] M. Suo, P. Wu, B. Zhou, An integrated method for interval multi-objective planning of a water resource system in the Eastern Part of Handan, Water Resour. Manage., 9 (2018) 528, doi: 10.3390/w9070528.
[4] J. Tian, S. Guo, D. Liu, A fair approach for multi-objective water resources allocation, Water Resour. Manage., 33 (2019) 363–365.
[5] R. Prasad, D. Sharma, K.D. Yadav, Preliminary study on effect of detention time on nutrient removal from greywater using water hyacinth, Water Conserv. Manage., 4 (2021) 20–25.
[6] E.E. Okon, J.O. Ikeh, C.J. Offodile, Near - surface characterization of sediments of the Sokoto group exposed around Wamakko area, Northwestern Nigeria: an integrated approach, Geol. Ecol. Landscapes, 5 (2021) 81–93.
[7] K.S. Rawat, S.K. Singh, S. Szilard, Comparative evaluation of models to estimate direct runoff volume from an agricultural watershed, Geol. Ecol. Landscapes, 5 (2021) 94–108.
[8] R.O.U. Eyankware, M.O. Eyankware, Contamination assessment of water resources around waste dumpsites in Abakaliki, Nigeria; A mini review, J. Clean WAS, 5 (2021) 17–20.
[9] K. Sie, T.J.H. Coulibaly, N. Coulibaly, I. Savane, L.D. Gone, K.C.A. Kouadio, H.S.J.P. Coulibaly, S. Cissé, I. Camara, G. Sylla, Contribution of satellite imagery to the characterization of the relationship between climate and pyrological variables of bush fires in the Savannah Zone (Case of the Bounkani Region), Environ. Ecosyst. Sci., 5 (2021) 64–72.
[10] S. Rijal, A review on soil conservation practices in Nepal, Environ. Contam. Rev., 3 (2020) 21–23.
[11] S. Khalid, Khanoranga, U. Altaf, R. Shah, G. Parveen, Drinking water quality assessment of Union Council Dhamni, Poonch, Azad Jammu And Kashmir, Pakistan, using water quality index and multivariate statistical analysis, Environ. Contam. Rev., 3 (2020) 24–31.
[12] K. Deb, H. Jain, An evolutionary many-objective optimization algorithm using reference-point-based nondominated sorting approach, Part I: Solving problems with box constraints, IEEE Trans. Evol. Comput., 18 (2018) 577–601.
[13] J.L. Expósito, M.V. Esteller, J. Paredes, C. Rico, R. Franco, Groundwater protection using vulnerability maps and wellhead protection area (WHPA): a case study in Mexico, Water Resour. Manage., 24 (2019) 421–422.
[14] J. L. Huang, Study on the characteristics of urban groundwater pollution and its control strategy, Environ. Sci. Manage., 18 (2020) 112–114.
[15] G.L. Yang, Study and discussion on nitrate pollution of urban groundwater, Eng. Res., 18 (2019) 57–60.
[16] J. Okkonen, R.M. Neupauer, Capture zone delineation methodology based on the maximum concentration: preventative groundwater well protection areas for heat exchange fluid mixtures, Water Resour. Res., 52 (2018) 404–406.
[17] R. Chmielewski, P. Muzolf, Selected problems of protection of historic buildings against the rainwater and the groundwater, MATEC Web Conf., 11 (2018) 176–178.
[18] M. Kang, R.B. Jackson, Salinity of deep groundwater in California: water quantity, quality, and protection, Proc. Natl. Acad. Sci. U.S.A., 113 (2016) 368–370.
[19] D. Machiwal, V. Cloutier, A review of GIS-integrated statistical techniques for groundwater quality evaluation and protection, Environ. Earth Sci., 77 (2019) 98–99.
[20] S. Saidi, D. Bouri, Assessment of groundwater risk using intrinsic vulnerability and hazard mapping: application to Souassi aquifer, Tunisian Sahel, Agric. Water Manage., 88 (2019) 66–67.
[21] J.T. He, Construction of groundwater pollution control zoning system, Environ. Sci., 11 (2018) 166–168.
[22] M.X. Li, Adjustment of industrial structure of resource-based cities based on prevention and control of groundwater pollution, Urban Dev. Res., 33 (2019) 66–70.